Internal Medicine
The Japanese Society of Internal Medicine
doi: 10.2169/internalmedicine.0521-22
Intern Med 62: 1335-1340, 2023
http://internmed.jp

【 CASE REPORT 】

Diffuse Large B-cell Lymphoma Involving an Abundant Infiltration of T Follicular Helper Cells

Keitaro Ishii[1], Kazuharu Kamachi[1,2], Sho Okamoto[1], Hiroo Katsuya[1], Mai Fujita[1], Toshiaki Nagaie[1], Atsujiro Nishioka[1], Mariko Yoshimura[1], Hiroshi Ureshino[1,2], Yasushi Kubota[1,3], Toshihiko Ando[1], Tatsuro Watanabe[2], Mai Takeuchi[4], Keita Kai[5], Koichi Ohshima[4] and Shinya Kimura[1,2]

Abstract:

A 76-year-old man presented with skin plaque and splenic nodules, and diffuse large B-cell lymphoma (DLBCL) with infiltration of T-cells was suspected based on the skin lesions. The disease showed indolent clinical behavior for three months, when systemic lymphadenopathy rapidly evolved. An inguinal lymph node biopsy revealed DLBCL with abundant infiltration of T follicular helper (TFH) cells. A polymerase chain reaction-based analysis of immunoglobulin variable heavy chain showed that the skin, splenic nodules, and inguinal lymph node shared the same clone. This case indicates that the dysregulated infiltration of TFH cells in the tumor microenvironment accelerates the lymphomagenesis and progression of DLBCL.

Key words: DLBCL, THRLBCL, T follicular helper cells

(Intern Med 62: 1335-1340, 2023)
(DOI: 10.2169/internalmedicine.0521-22)

Introduction

Diffuse large B-cell lymphoma (DLBCL), the most common subtype of non-Hodgkin lymphoma, has clinically and biologically heterogenous features. Although rituximab, cyclophosphamide, doxorubicin, vincristine, and prednisone (R-CHOP) immunochemotherapy leads to a cure in approximately 60% of DLBCL patients (1), relapsed or refractory DLBCL patients have a poor outcome. In an effort to achieve better therapeutic and prognostic stratification of DLBCL, the tumor microenvironment (TME) has recently received attention, in addition to the biological features of DLBCL (2, 3).

T-cell/histiocyte-rich large B-cell lymphoma (THRLBCL) is a variant of DLBCL characterized by TME with an extensive infiltrate of several subsets of T-cells and histiocytes (4). THRLBCL develops with maintaining a tolerogenic host immune response (5), while the interaction between TME and B-cells in lymphomagenesis remains unclear. T follicular helper (TFH) cells, a subset of helper T-cells, support the maturation of B-cells in the germinal center of lymphoid tissues (6, 7) and express specific TFH markers, such as PD-1, ICOS, and CXCR5. Dysregulation of TFH cells causes autoimmunity, immunodeficiency, and malignant lymphoma, especially angioimmunoblastic T-cell lymphoma (AITL) (8), presumably playing a pivotal role in TME.

We herein report a unique case showing the stepwise progression of DLBCL in accordance with infiltration of TFH cells. Increased infiltration of TFH cells pathologically mimicked AITL and led to rapid progression of DLBCL.

Case Report

A 76-year-old man with chronic hepatitis B infection pre-

[1]Division of Hematology, Respiratory Medicine and Oncology, Department of Internal Medicine, Faculty of Medicine, Saga University, Japan, [2]Department of Drug Discovery and Biomedical Sciences, Faculty of Medicine, Saga University, Japan, [3]Department of Transfusion Medicine and Cell Therapy, Saitama Medical Center, Saitama Medical University, Japan, [4]Department of Pathology, Kurume University School of Medicine, Japan and [5]Department of Pathology, Saga University Hospital, Japan
Received: June 20, 2022; Accepted: August 3, 2022; Advance Publication by J-STAGE: September 21, 2022
Correspondence to Dr. Kazuharu Kamachi, kazuharu86@gmail.com

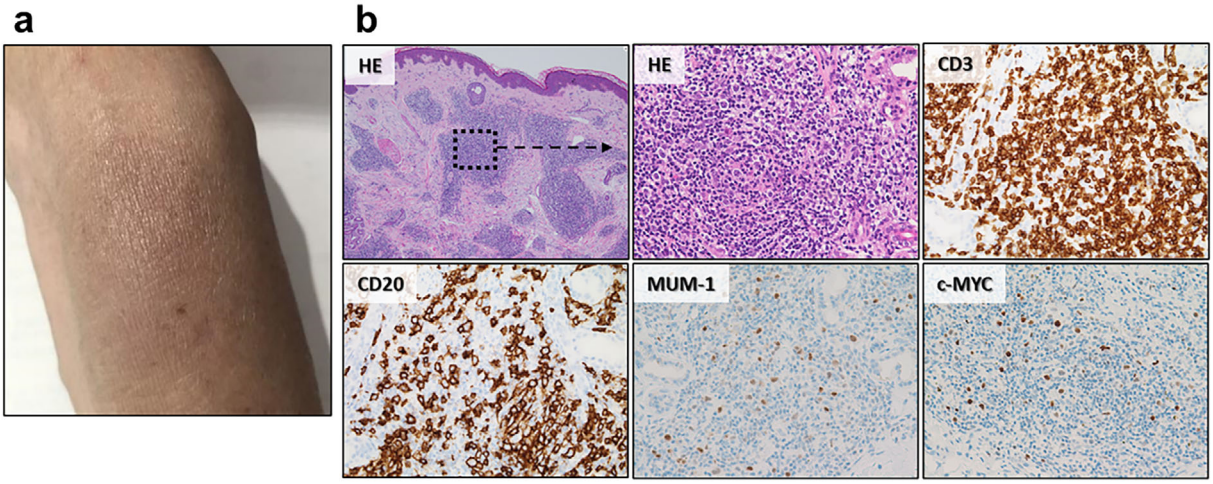

Figure 1. The skin lesion showed B-cell lymphoma with abundant T-cell infiltration. (a) An image of the skin plaque on the left forearm with a brownish-red color appearance. (b) Immunopathological findings of the skin lesion are shown. Hematoxylin and Eosin (HE) staining showed nodular proliferation of small to large lymphocytes, mainly in the subcutaneous adipose tissue (left upper image, original magnification ×40). The large lymphocytes were positive for CD20, MUM-1 (focal), and c-MYC (focal), with abundant infiltration of $CD3^+$T cells (magnified images of the area with the dotted square; original magnification ×200).

sented with splenic nodules and isolated para-aortic lymphadenopathy incidentally detected during an annual ultrasonography and computed tomography study. The patient had no systemic symptoms, such as a fever, weight loss, or night sweats.

The patient reported noticing a slow-growing skin plaque on the left forearm approximately one year earlier (Fig. 1a). Laboratory tests showed normal blood cell counts with an elevated level of soluble interleukin 2 receptor (sIL-2R) (1,484 U/L; reference range, 121-613 U/L), and monoclonal IgM gammopathy (696 mg/dL; reference range, 33-183 mg/dL). Esophagogastroduodenoscopy and total colonoscopy detected no malignancy. Positron emission tomography/computed tomography showed the uptake of the glucose analog ^{18}F-fluorodeoxyglucose in the skin lesion and in the right inguinal lymph node, as well as a subcutaneous lesion in the right thigh, each <2.0 cm in diameter.

Because malignancies were clinically suspected, splenectomy, a skin biopsy, and a para-aortic lymph node biopsy were performed. The spleen showed a non-specific inflammatory pseudotumor. The para-aortic lymph node showed reactive lymphoid hyperplasia. A skin plaque biopsy showed nodular expansion of large B cells ($CD20^+$, c-MYC^+, MUM-1^+, $EBER^-$) surrounded by abundant infiltration of $CD3^+$ T cells. This led to the diagnosis of DLBCL with abundant T-cell infiltration (Fig. 1b).

A bone marrow examination showed no obvious infiltration of abnormal lymphocytes; however, slightly λ-dominated light-chain restriction and chromosomal abnormalities [46,XY,add(12)(p13),-14,-16,+der(?)t(?;14)(?;q11.2),+mar1(2)/46,XY(18)] were detected by flow cytometry and a G-banding analysis, respectively, implying bone marrow invasion of B-cell lymphoma. Circulating Epstein-Barr virus (EBV) DNA was not detected by quantitative polymerase chain reaction (PCR). The asymptomatic and indolent presentation led us to follow the patient carefully without initiating chemotherapy.

Three months later, a flow cytometry analysis showed the gradual emergence of peripheral abnormal lymphocytes and clonal B cells ($CD20^+$, λ>κ) concurrent with an elevated level of sIL-2R. Although the skin lesion showed fading, systemic lymphadenopathy rapidly developed, and a left inguinal lymph node biopsy showed diffuse infiltration of both large B cells ($CD20^+$, c-MYC^+, MUM-1^+, $EBER^-$) and $CD4^+$ T cells expressing TFH markers (PD-1^+, $ICOS^+$, $CXCR5^+$, $CXCL13^+$) with an expanded follicular dendritic cell meshwork (Fig. 2a, b), suggesting composite AITL and DLBCL. $EBER^+$ B cells were detected in some small non-malignant B cells, and circulating EBV DNA was elevated (3.6 log IU/mL). A G-banding analysis showed [46,XY,del(6)(p?),add(12)(p13),-14,add(14)(q32),-16,+mar1,+mar2(14)/46,XY(6)].

The patient achieved complete metabolic remission after six cycles of R-CHOP chemotherapy. However, three months later, he experienced relapse with bilateral tonsillar enlargement, and DLBCL was confirmed by a tonsil biopsy. Polatuzumab vedotin, bendamustine, and rituximab (Pola-BR) immunotherapy was then commenced as salvage therapy. The overall clinical course is illustrated in Fig. 3a.

A Southern blot analysis of immunoglobulin variable heavy chain (IGVH) and T-cell receptor (TCR) β-chain and a PCR-based analysis of the TCR γ-chain gene of the inguinal lymph node showed no clonal rearrangements, and the *RHOA* G17V mutation, as well as *MYD88* L265P mutation, was undetected. The PCR-based analysis of IGVH showed that the skin lesion, spleen nodules, peripheral blood cells with abnormal lymphocytes, inguinal lymph node, and tonsil

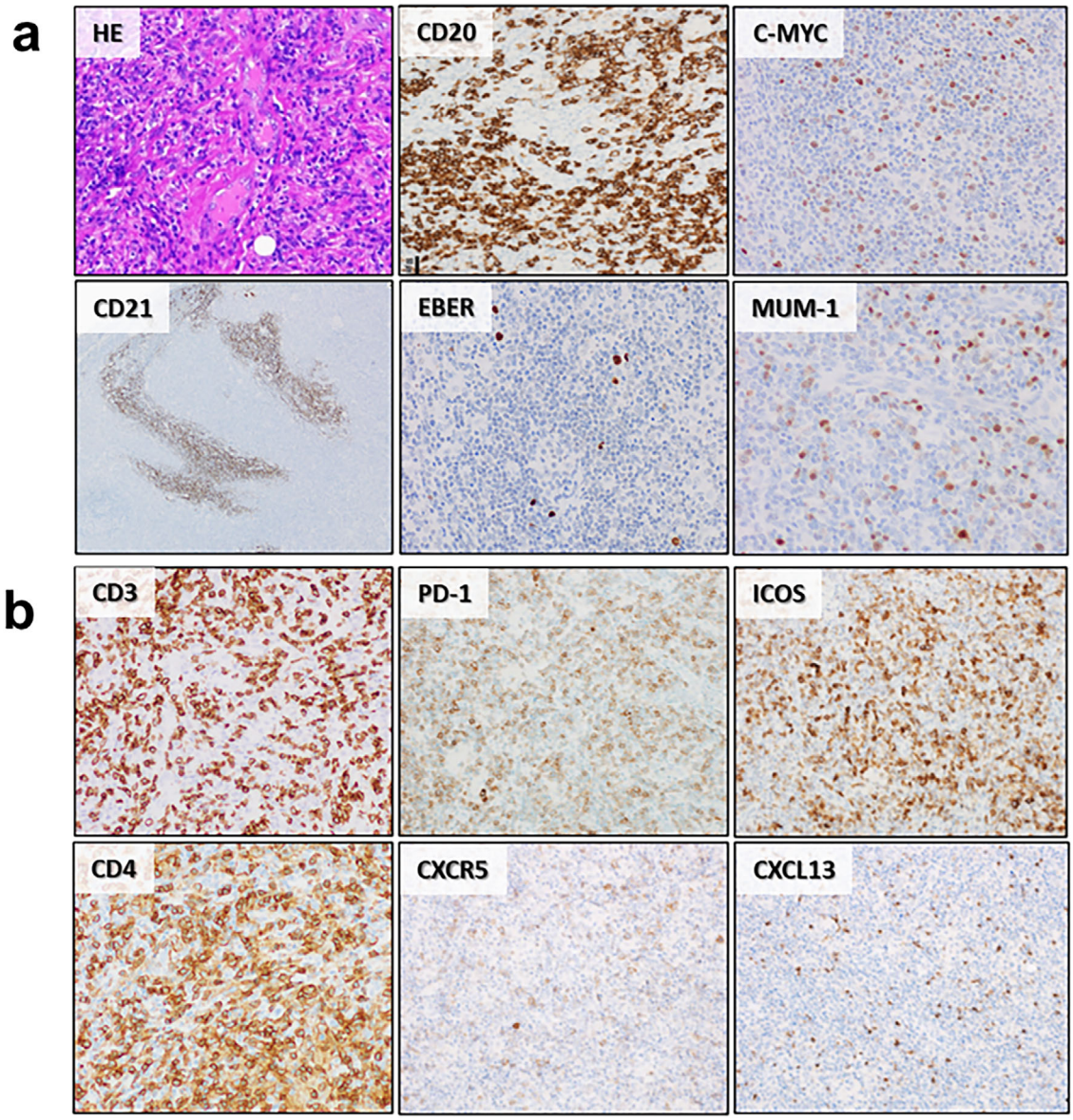

Figure 2. **Immunopathological findings of the inguinal lymph node showing composite AITL and DLBCL. (a) Hematoxylin and Eosin staining showed diffuse proliferation of small to large atypical lymphocytes in the background of expanded high endothelial venules and a follicular dendritic cell meshwork (CD21). The large lymphocytes expressed CD20, c-MYC (focal), and MUM-1 (focal), whereas EBER was detected in the background small lymphocytes. (b) The small to medium-sized lymphocytes with nuclear atypia were mainly positive for CD3, CD4, PD-1, and ICOS and partially positive for CXCR5 and CXCL13 (original magnification ×200, except for CD21 ×40).**

shared the same clonal band, suggesting the progression of the same clone (Fig. 3b). Consistently, $CD20^+$ and $MUM\text{-}1^+$ large B cells were detected in the spleen nodules, and infiltration of T cells expressing TFH markers was detected in both the spleen and the skin lesion (Fig. 4a, b). Furthermore, the remarkably increased infiltration of $PD\text{-}L1^+$ cells, including large tumor cells and tumor-associated macrophages (TAMs), was observed in the inguinal lymph node compared with the skin and splenic nodules (Fig. 4c).

Methods

The PCR analysis of IGVH gene rearrangement

Genomic DNA was extracted from each sample (skin lesion, spleen nodule, peripheral mononuclear cells, inguinal lymph node, and tonsil lesion) using a QIAamp DNA Mini Kit (Qiagen, Venlo, Netherlands). The B-cell clonality of each sample was analyzed by the nested PCR method to detect IGVH gene rearrangement. The following primers were commercially synthesized: FR3A (5'-ACACGGCSSTGTATTACTGT-3'), LJH (5'-TGAGGAGACGGTGACC-3'), and VLJH (5'-GTGACCAGGGTNCCTTGGCCCCAG-3'). FR3A and LJH were used as the initial PCR primers, and FR3A and VLJH were used as the secondary PCR primers (9). Electrophoresis of PCR products was performed with a 12% acrylamide gel. The Burkitt lymphoma-derived cell line Raji (Japanese Collection of Research Bioresources

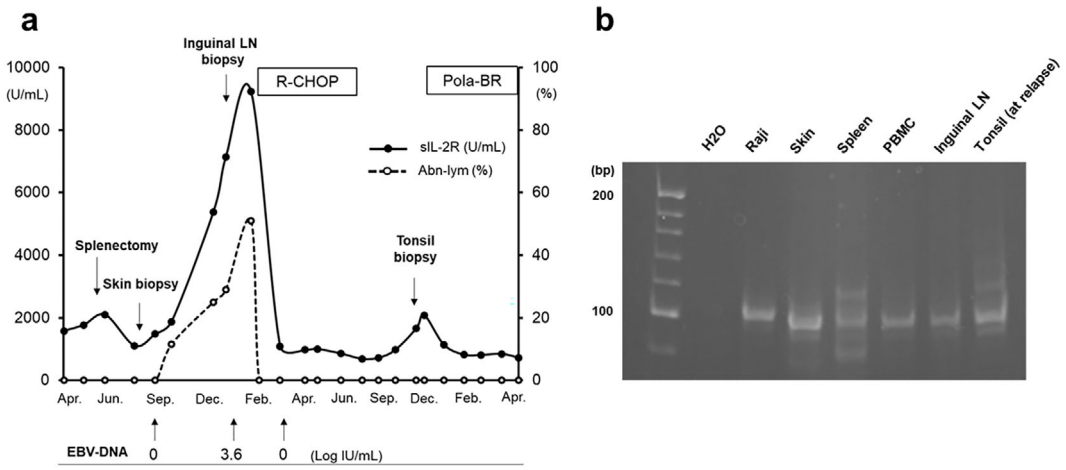

Figure 3. The overall clinical course and PCR analysis findings of somatic mutations in IGVH genes. (a) The overall clinical course is illustrated. Solid and dotted lines show the transition of soluble interleukin 2 receptor (sIL-2R, U/mL) and abnormal lymphocytes (%) in peripheral blood, respectively. Quantification of circulating Epstein-Barr virus DNA (EBV DNA) at each time point and the duration of chemotherapy (R-CHOP and Pola-BR) are also noted. (b) The findings concerning somatic mutations in IGVH genes are shown. The Burkitt lymphoma-derived cell line Raji and H_2O were used as positive and negative controls of IGVH gene rearrangement, respectively. The skin lesion (Skin), spleen nodules (Spleen), peripheral blood mononuclear cells (PBMCs), inguinal lymph node (Inguinal LN), and tonsil lesion (at relapse) shared the same clonal band, just below 100 bp.

Cell Bank, ibaraki, Japan) was used as the positive control for IGVH gene rearrangement (Fig. 3b).

Discussion

We herein report a unique case of DLBCL that showed stepwise progression in accordance with the increased infiltration of TFH cells. The transition to rapid progressive DLBCL manifesting as leukemic emergence of malignant B cells and rapid increase of sIL-2R levels was observed, consistent with the increased infiltration of TFH cells. The absence of the *MYD88* L265P mutation negated the possibility of DLBCL transformation from lymphoplasmacytic lymphoma. The presence of $EBER^+$ B cells in the inguinal lymph node, accompanied by increased levels of circulating EBV DNA, suggested attenuated cellular immunity. A PCR-based analysis of IGVH showed the clonal progression of B-cell lymphoma, and an immunohistochemical analysis revealed that the progression of B-cell lymphoma was accompanied by infiltration of TFH cells and $PD\text{-}L1^+$ cells, including large tumor cells and TAMs.

The first presentation in the present case was a skin plaque, which prompted us to suspect primary cutaneous large B-cell lymphoma (PCLBCL), leg type, given the rapid systemic progression and early relapse after conventional treatment. However, a skin biopsy showed nodular expansion of large B cells surrounded by abundant infiltration of $CD3^+$ T cells, which is inconsistent with typical PCLBCL, leg type, being characterized by diffuse dermal infiltration of large B cells with minimal reactive T component (10). Therefore, we considered PCLBCL, leg type, to be unlikely in the present case.

The pathological findings of the inguinal lymph node showed diffuse infiltration of both large B cells and TFH cells, mimicking composite AITL and DLBCL. AITL has diverse clinical and histopathological manifestations, and it is sometimes difficult to distinguish from benign immune reactions and other malignant lymphomas (11). The present patient lacked constitutional symptoms and autoimmune complications, which are relatively common in AITL patients. The PCR-based analysis did not detect TCR γ-chain gene rearrangement, indicating a non-clonal proliferation. Furthermore, the *RHOA* G17V mutation, which is specific to AITL and nodal peripheral T-cell lymphoma with TFH phenotype, was also not detected (12, 13). Given that the infiltration of TFH cells is consistently observed during the progression of B-cell lymphoma, we may reasonably assume that an "AITL-like manifestation" occurred against the progression of B-cell lymphoma.

The TME that recruited additional TFH cells around B cells may have been associated with lymphomagenesis in the present case. TFH markers are occasionally expressed in background T cells in THRLBCL (14); however, their significance remains unclear. TFH cells originally interact with B cells and support the migration and differentiation of B cells in germinal centers of lymph nodes (6, 7). During this process, TFH cells also become polarized to express additional TFH markers, such as PD-1 and CXCR5 (15). Furthermore, TFH cells support the survival of malignant B cells in follicular lymphoma (16). In AITL, in which TFH cells clonally expand, EBV reactivation and subsequent monoclonal or oligoclonal expansion of B cells are fre-

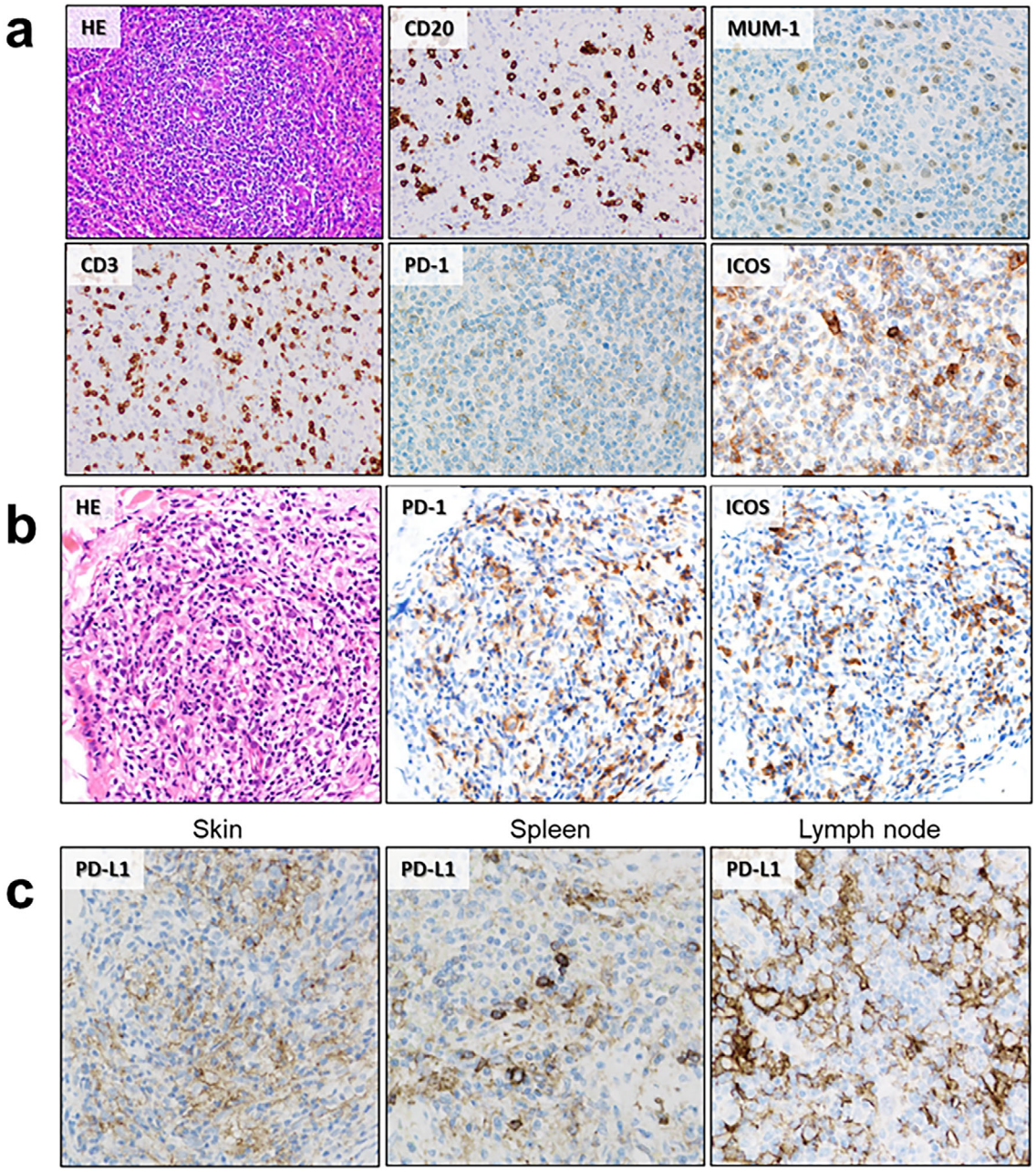

Figure 4. **Immunopathological findings of the spleen nodules, the skin lesion, and PD-L1 staining of each specimen. (a) Hematoxylin and Eosin staining of the spleen nodule showed increased fibrosis with partial vitrification in the background of inflammatory cell infiltration. Immunostaining revealed scattered infiltration of large CD20$^+$ and MUM-1$^+$ atypical cells, in addition to the surrounding infiltration of CD3$^+$, PD-1$^+$, and ICOS$^+$ cells. (b) Immunopathological findings of the skin lesion are shown. There is abundant infiltration of PD-1$^+$ and ICOS$^+$ cells. (c) PD-L1 immunostaining of each specimen (skin, spleen, and lymph node) is shown. Numerous infiltrations of PD-L1$^+$ cells, including large tumor cells and tumor-associated macrophages, were observed in each specimen, especially in the lymph node (original magnification ×200).**

quently observed (17). Thus, TFH-infiltrating THRLBCL may have a similar pathogenesis associated with AITL.

Another intriguing aspect of the present case was that the increased infiltration of PD-L1$^+$ cells, including large tumor cells and TAMs, was observed in the inguinal lymph node compared with the skin and splenic nodules. The direct contact between PD-L1$^+$ TAMs and the surrounding T cells promotes immune evasion and lymphomagenesis by increasing the PD-1/PD-L1 interaction in TME (18, 19). Recent studies have shown that THRLBCL frequently harbors PD-L1/PD-L2 alterations, which leads to increased PD-L1 expression, and the TME in THRLBCL is characterized by the presence of abundant PD-1$^+$ T cells and PD-L1$^+$ TAMs, resulting in ineffective immune cell infiltration (20, 21). Ac-

cording to these reports, immune evasion via PD-1/PD-L1 interaction, which can be promoted by PD-L1$^+$ tumor cells and infiltration of PD-L1$^+$ TAMs, may have triggered and accelerated the development of DLBCL in the present case.

In summary, we described a unique case showing the stepwise progression of DLBCL in accordance with the infiltration of TFH cells. This case indicates that the dysregulated infiltration of TFH cells in TME plays a crucial role in the progression of DLBCL. TFH-infiltrating THRLBCL may develop and progress with disruption of immune surveillance, such as PD-1/PD-L1 interaction. The analysis of a greater number of DLBCL cases is needed to elucidate the pathological significance of TFH cells in the TME and its relevance to clinical outcomes.

Informed Consent

Informed consent was obtained from the patient for publication of this case report.

Author's disclosure of potential Conflicts of Interest (COI).

Shinya Kimura: Research funding, Chugai Pharmaceutical.

References

1. Coiffier B, Thieblemont C, Van Den Neste E, et al. Long-term outcome of patients in the LNH-98.5 trial, the first randomized study comparing rituximab-CHOP to standard CHOP chemotherapy in DLBCL patients: a study by the Groupe d'Etudes des Lymphomes de l'Adulte. Blood **116**: 2040-2045, 2010.
2. Sehn LH, Salles G. Diffuse Large B-cell lymphoma. N Engl J Med **384**: 842-858, 2021.
3. Miyawaki K, Kato K, Sugio T, et al. A germinal center-associated microenvironmental signature reflects malignant phenotype and outcome of DLBCL. Blood Adv **6**: 2388-2402, 2022.
4. Arber DA, Orazi A, Hasserjian R, et al. The 2016 revision to the World Health Organization classification of myeloid neoplasms and acute leukemia. Blood **127**: 2391-405, 2016.
5. VanLoo P, Tousseyn T, Vanhentenrijk V, et al. T-cell/histiocyte-rich large B-cell lymphoma shows transcriptional features suggestive of a tolerogenic host immune response. Haematologica **95**: 440-448, 2010.
6. Crotty S. A brief history of T cell help to B cells. Nat Rev Immunol **15**: 185-189, 2015.
7. Crotty S. T follicular helper cell differentiation, function, and roles in disease. Immunity **41**: 529-542, 2014.
8. Shekhar S, Yang X. The darker side of follicular helper T cells: from autoimmunity to immunodeficiency. Cell Mol Immunol **9**: 380-385, 2012.
9. Van Dongen JJ, Langerak AW, Brüggemann M, et al. Design and standardization of PCR primers and protocols for detection of clonal immunoglobulin and T-cell receptor gene recombinations in suspect lymphoproliferations: report of the BIOMED-2 Concerted Action BMH4-CT98-3936. Leukemia **17**: 2257-2317, 2003.
10. Vitiello P, Sica A, Ronchi A, et al. Primary cutaneous B-cell lymphomas: an update. Front Oncol **10**: 651, 2020.
11. Xie Y, Jaffe ES. How I Diagnose angioimmunoblastic T-cell lymphoma. Am J Clin Pathol **156**: 1-14, 2021.
12. Sakata-Yanagimoto M, Enami T, Yoshida K, et al. Somatic *RHOA* mutation in angioimmunoblastic T cell lymphoma. Nat Genet **46**: 171-175, 2014.
13. Palomero T, Couronné L, Khiabanian H, et al. Recurrent mutations in epigenetic regulators, *RHOA* and *FYN* kinase in peripheral T cell lymphomas. Nat Genet **46**: 166-170, 2014.
14. Abukhiran I, Syrbu SI, Holman CJ. Markers of follicular helper T cells are occasionally expressed in T-cell or histiocyte-rich large B-cell lymphoma, classic hodgkin lymphoma, and atypical paracortical hyperplasiaa diagnostic pitfall for T-cell lymphomas of T follicular helper origin. Am J Clin Pathol **156**: 409-426, 2021.
15. Baumjohann D, Brossart P. T follicular helper cells: linking cancer immunotherapy and immune-related adverse events. J Immunother Cancer **9**: e002588, 2021.
16. Amé-Thomas P, Le Priol J, Yssel H, et al. Characterization of intratumoral follicular helper T cells in follicular lymphoma: role in the survival of malignant B cells. Leukemia **26**: 1053-1063, 2012.
17. Kawano R, Ohshima K, Wakamatsu S, Suzumiya J, Kikuchi M, Tamura K. Epstein-Barr virus genome level, T-cell clonality and the prognosis of angioimmunoblastic T-cell lymphoma. Haematologica **90**: 1192-1196, 2005.
18. Carey CD, Gusenleitner D, Lipschitz M, et al. Topological analysis reveals a PD-L1-associated microenvironmental niche for Reed-Sternberg cells in Hodgkin lymphoma. Blood **130**: 2420-2430, 2017.
19. Le K, Sun J, Khawaja H, et al. Mantle cell lymphoma polarizes tumor-associated macrophages into M2-like macrophages, which in turn promote tumorigenesis. Blood Adv **5**: 2863-2878, 2021.
20. Godfrey J, Tumuluru S, Bao R, et al. *PD-L1* gene alterations identify a subset of diffuse large B-cell lymphoma harboring a T-cell-inflamed phenotype. Blood **133**: 2279-2290, 2019.
21. Griffin GK, Weirather JL, Roemer MGM, et al. Spatial signatures identify immune escape via PD-1 as a defining feature of T-cell/histiocyte-rich large B-cell lymphoma. Blood **137**: 1353-1364, 2021.